Anusandhanvallari
Vol 2024, No.1
August 2024
ISSN 2229-3388

Microwave-Enabled Synthesis of Dihydropyrazolo[4',3':5,6]pyrano[2,3-d]pyrimidine Derivatives Utilizing Hf based Magnetic–Metal Organic Frameworks (MMOFs) - Fe3O4@SiO2@UiO-66 (Hf) as Heterogeneous Catalysts

Mr. S. P. Gawali[a,b*], Mrs. S. S. Kamble[a], Dr. Prof. D. V. Mane[c,d]

[a]Department of Chemistry, Sundarrao More Arts, Commerce and Science College, Poladpur, Raigad, 402303 India

[b]School of Science, Yashwantrao Chavan Maharashtra open University, Nashik, Maharashtra 402222 India

[a]Department of Chemistry, Sundarrao More Arts, Commerce and Science College, Poladpur, Raigad, 402303 India

[c]Former. Regional Director, YCMOU Nashik 402222 India

[d]Department of Chemistry, Shri Chhatrapati Shivaji College Omerga, Dharashiv 413606 India

Abstract

A novel, efficient, and green synthetic protocol for dihydropyrazolo[4',3':5,6]pyrano[2,3-d]pyrimidine derivatives was developed using microwave irradiation and a magnetic–metal organic framework (MMOF) catalyst, Fe_3O_4@SiO_2@UiO-66(Hf). The catalyst, synthesized via a stepwise approach, combines the magnetic properties of Fe_3O_4 with the robust, porous UiO-66 (Hf) framework, enabling facile separation and reuse. Characterization techniques including X-ray diffraction (XRD), Fourier-transform infrared spectroscopy (FT-IR), scanning electron microscopy (SEM), and EDX analysis confirmed the successful fabrication of the MMOF. The identification of the product compounds was achieved through spectral analysis of dihydropyrazolo[4',3':5,6]pyrano[2,3-d]pyrimidine derivatives, employing ^{1}H NMR, ^{13}C NMR, and IR spectroscopy. The catalytic system demonstrated high efficiency under microwave irradiation, affording excellent yields (85–94%) within very short reaction times (6 min) under solvent-free conditions. Optimization studies revealed the optimal catalyst loading and microwave power for maximum conversion. The catalyst exhibited remarkable recyclability, retaining activity over five consecutive cycles with minimal loss. Comparative studies highlighted superior performance over conventional catalysts in terms of reaction rate and environmental sustainability. Mechanistic investigations suggest a cooperative activation of substrates via Lewis acidic Hf sites and microwave-induced heating, promoting rapid cyclization. This heterogeneous catalytic approach aligns with principles of green chemistry, offering an expedient, recyclable, and environmentally benign route to valuable heterocyclic scaffolds with potential applications in medicinal chemistry.

Keywords: Dihydropyrazolopyranopyrimidines; Magnetic Metal–Organic Frameworks; UiO-66(Hf); Microwave-Assisted Synthesis; Heterogeneous Catalysis; Green Chemistry; Catalyst Recyclability

1. Introduction

Dihydropyrimidine-based heterocycles represent a significant class of nitrogen-containing compounds with diverse biological activities, including antiviral [1], anticancer [2, 4], and anti-inflammatory properties [3].

Among these, fused heterocyclic systems such as dihydropyrazolo[4',3':5,6]pyrano[2,3-d]pyrimidines have attracted considerable attention due to their structural complexity and potential as pharmacophores [4]. Traditional synthetic methods for these compounds often involve multistep procedures, harsh conditions, and homogeneous catalysis, which limit sustainability and scalability [5,6].

The development of green and heterogeneous catalytic systems has emerged as a pivotal strategy to address these challenges. Heterogeneous catalysts offer advantages such as easy separation, recyclability, and reduced environmental impact [7]. Metal–organic frameworks (MOFs), with their tunable porosity, high surface area, and structural versatility, have become prominent candidates in heterogeneous catalysis [8]. Particularly, hafnium-based MOFs (UiO-66(Hf)) exhibit exceptional thermal and chemical stability, as well as Lewis acidity, favorable for catalyzing a variety of organic transformations [9].

Incorporating magnetic nanoparticles (Fe3O4) into MOFs to form magnetic–metal organic frameworks (MMOFs) further enhances catalyst recovery via magnetic separation, aligning with eco-friendly process design [10, 11]. Despite advances, the application of Hf-based MMOFs in microwave-assisted synthesis of fused heterocycles remains underexplored.

This study addresses this gap by developing a microwave-facilitated, heterogeneous catalytic method employing Fe3O4@SiO2@UiO-66(Hf) MMOFs for the synthesis of dihydropyrazolo[4',3':5,6]pyrano[2,3-d]pyrimidine derivatives. The approach aims to combine the benefits of microwave irradiation and MMOF catalysis to achieve rapid, efficient, and green synthesis of these valuable heterocycles.

2. Materials and Methods

2.1 Chemicals and Reagents

All chemicals were of analytical grade and used without further purification. Hafnium(IV) chloride (HfCl4), terephthalic acid, iron(III) chloride hexahydrate ($FeCl_3 \cdot 6H_2O$), iron(II) chloride tetrahydrate ($FeCl_2 \cdot 4H_2O$), sodium meta silicate (Na_2SiO_3), ammonium hydroxide, and other organic substrates were procured from standard suppliers.

2.2 Synthesis of Fe_3O_4@SiO_2@UiO-66 (Hf) MMOFs

2.2.1 Synthesis of Fe_3O_4

Magnetic magnetite (Fe_3O_4) nanoparticles are produced through the chemical co-precipitation of ferric (Fe^{3+}) and ferrous (Fe^{2+}) ions. Iron (III) chloride hexahydrate and iron(II) chloride tetrahydrate are dissolved in deionized water, maintaining a 2:1 ratio of Fe^{3+} to Fe^{2+}. Hydrochloric acid is added to prevent the early formation of hydroxides. Mercaptoethanol acts as a stabilizer, and the system is deoxygenated using nitrogen at 80°C. The addition of ammonium hydroxide while stirring causes the solution to turn black. Microwave irradiation is then used to crystallize the nanoparticles, which are subsequently collected through centrifugation and dried to yield Fe_3O_4 nanoparticles.

2.2.2 Synthesis of Fe_3O_4@SiO_2

The $Fe_3O_4@SiO_2$ composite was created by subjecting Fe_3O_4 nanoparticles to microwave heating in distilled water combined with a sodium silicate solution. This synthesis employs a modified Stöber method, which involves depositing SiO_2 onto Fe_3O_4 nanoparticles. Initially, the Fe_3O_4 nanoparticles are dispersed in a mixture of water and ethanol and then subjected to ultrasonication. The pH is increased to 11 using NaOH, after which a sodium metasilicate solution is introduced. Subsequently, the pH is adjusted to 9 with HCl to facilitate the

formation of the SiO_2 shell. Following microwave irradiation and an overnight aging process, the $Fe_3O_4@SiO_2$ nanoparticles are washed, magnetically collected, and dried.

2.2.3 Synthesis of Hf-UiO-66

Synthesis of Hf-UiO-66 involves a solvothermal approach using hafnium tetrachloride ($HfCl_4$) and 1,4-benzenedicarboxylic acid (H_2BDC). $HfCl_4$ reacts with H_2BDC to form the hafnium-oxo cluster $[Hf_6O_4(OH)_4(BDC)_6]$, the framework's secondary building unit. The synthesis occurs in N,N-dimethylformamide (DMF) with hydrochloric acid (HCl) as modulator for crystal growth. The mixture is heated under microwave irradiation at 80 ^{0}C with 700 W powers for few minute to form the MOF structure.

2.2.4 Synthesis of Hf-MMOF ($Fe_3O_4@SiO_2$-UiO-66-Hf)

It begins by dispersing 1.0 g of $Fe_3O_4@SiO_2$ in 45 mL DMF and ultrasonicating for 30 minutes. Then, 2 mmol $HfCl_4$ (0.5567 g) is added with 10 minutes ultrasonication. 2 mmol H2BDC (0.332 g) dissolved in 10 mL DMF and 0.9 mL HCl are added. The solution is microwave-heated at 80 ^{0}C for 8 minutes at 700 W, followed by 12 hours reaction. The product is washed with DMF for 5 time and separated by strong external magnet and dried at 50 ^{0}C for 24 hours to obtain Hf-MMOF composite **($Fe_3O_4@SiO_2$-UiO-66-Hf)**

2.3 Catalyst Characterization

XRD patterns were recorded to confirm crystallinity and phase purity of the MMOF composite.

FT-IR spectra were obtained to identify characteristic functional groups and confirm successful MOF formation. **SEM** imaging provided morphological details and particle size distribution.

2.4 General Procedure for Synthesis of Dihydropyrazolo[4',3':5,6]pyrano[2,3-d]pyrimidine Derivatives

In a solvent-free environment, a blend of ethyl acetoacetate, hydrazine hydrate, an aromatic aldehyde, and barbituric acid, each measuring 10 mmol, was combined with 0.1 g of the Hf-MMOF ($Fe_3O_4@SiO_2$-UiO-66-Hf) catalyst. This mixture was exposed to microwave irradiation at a power of 450 W for duration of 6 minutes, with its progress being monitored through TLC. After the reaction mixture was allowed to cool, ethanol was used to extract the product, and the catalyst was separated by filtration. The resulting solution was concentrated, and pure dihydropyrazolo[4',3':5,6]pyrano[2,3-d]pyrimidine derivatives were obtained by recrystallizing from ethanol.

3. Results

3.1 Catalyst Characterization

3.1.1 X-ray Diffraction (XRD) Analysis

Figure 1 illustrates the XRD analysis of crystalline structures, confirming the successful creation of Fe3O4, Fe3O4@SiO2, UiO-66, and Fe3O4@SiO2@UiO-66 nanoparticles. The XRD pattern for Fe3O4 verifies its characteristic magnetic iron oxide crystal structure [12, 13]. When Fe3O4 is coated with SiO2, forming Fe3O4@SiO2, the XRD peaks of Fe3O4 remain visible, though they might appear slightly diminished or broadened due to the silica coating [13, 14]. The characterization peaks align well with the UiO-66 crystalline structure as documented in existing literature [15]. In the composite Fe3O4@SiO2-UiO-66 (Hf), the XRD pattern displays features from both the Fe3O4@SiO2 core and the UiO-66 shell, demonstrating that the composite material retains the crystal structures of both components.

Anusandhanvallari
Vol 2024, No.1
August 2024
ISSN 2229-3388

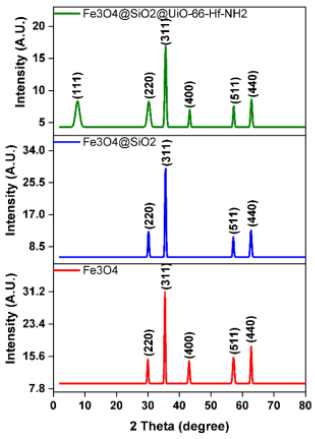

Figure 1. PXRD spectra of Fe_3O_4, Fe_3O_4@SiO_2 and Fe_3O_4@SiO2-UiO-66 (Hf)

3.1.2 Fourier Transform Infrared Spectroscopy (FTIR):

Figure 2 illustrates the use of FTIR spectroscopy to investigate the structural properties of the synthesized magnetic nanoparticles. The detection of two distinct peaks at 533 and 1028 cm^{-1} verifies the formation of silica-coated magnetic nanoparticles, corresponding to the stretching vibrations of Fe-O and Si-O, respectively. The absorption peaks observed at 1389 and 1690 cm-1 are linked to C=C and C=O bonds, signifying the successful attachment of MPS to the silica-coated magnetic Fe_3O_4 nanoparticles [16, 17]. Additionally, the FTIR spectra displayed all characteristic peaks of UiO-66 and Fe_3O_4@UiO-66, including the out-of-plane and in-plane stretching modes of –COO- groups at 1398 and 1577 cm-1, the symmetric and asymmetric stretching vibrations of carboxylic functional groups between 1350-1700 cm-1, the stretching vibrations of aliphatic and aromatic C-H bonds from 2932-3100 cm-1, and the stretching vibrations of oxygen-hydrogen bonds ranging from 3250-3600 cm-1 [18]. These results confirm that UiO-66 was effectively grown on the surface of the functionalized Fe3O4 nanoparticles.

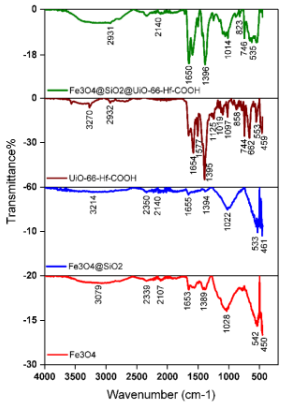

Figure 2 FTIR spectra of Fe_3O_4, Fe_3O_4@SiO_2, UiO-66 (Hf), and Fe_3O_4@SiO2-UiO-66 (Hf)

3.1.3 Scanning Electron Microscopy (SEM):

The SEM images (fig. 3) show morphological evolution across synthesis stages. The pristine Fe_3O_4 nanoparticles display uniform spherical morphology with smooth surfaces. After silica coating to form $Fe_3O_4@SiO_2$, particles maintain spherical shape but show increased surface roughness [16, 19]. The UiO-66-Hf-based MMOFs exhibit octahedral crystalline structures with well-defined faceted surfaces, where functional groups influence crystal size and surface morphology while maintaining octahedral geometry [19, 20]. SEM images indicated uniform spherical morphology with particle sizes around 150 nm.

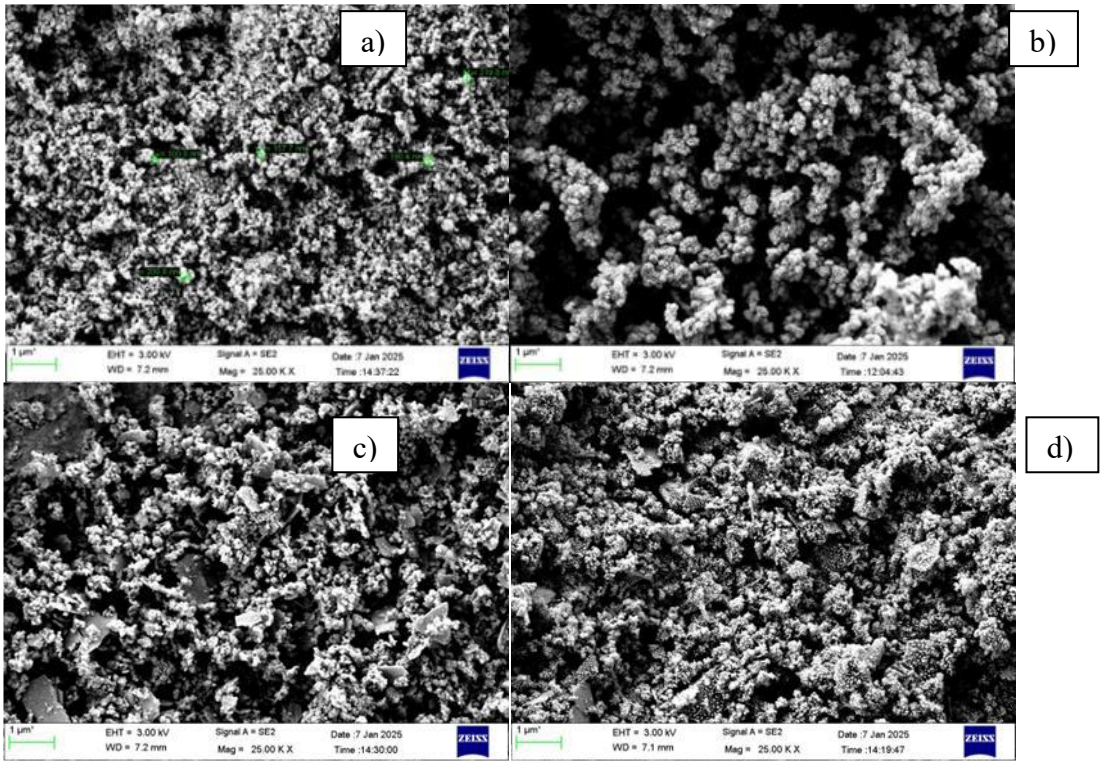

Figure 3. SEM Images of a) Fe_3O_4 b) $Fe_3O_4@SiO_2$ c) UiO-66 (Hf) d) Fe_3O_4@SiO2-UiO-66 (Hf)

3.1.4 Elemental Analysis (EDX)

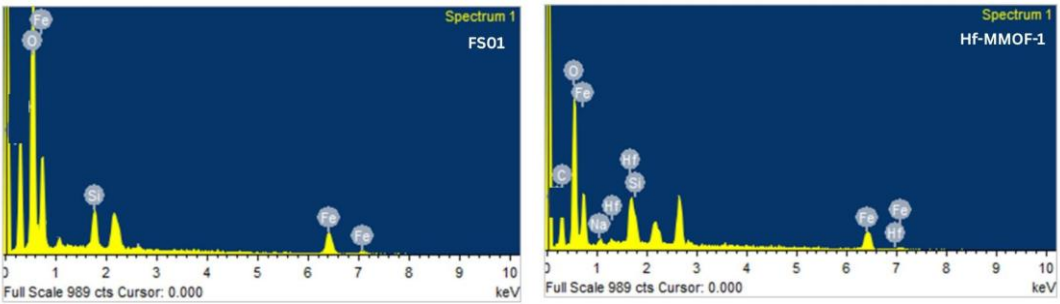

Figure 4. EDX pattern of a) $Fe_3O_4@SiO_2$ b) Fe_3O_4@SiO2-UiO-66 (Hf)

The EDX spectra depicted in Fig 4 verify the presence of Fe, O, Si, and Hf elements within the samples, demonstrating the successful synthesis of Fe_3O_4, Fe3O4@SiO2, UiO-66 (Hf), and Fe3O4@SiO2-UiO-66 (Hf). In Fe3O4 and Fe3O4@SiO2, the signals for Fe and O are predominant, while the Si peak becomes more pronounced following the silica coating [21]. For UiO-66 (Hf) and Fe3O4@SiO2-UiO-66 (Hf), the detection of Hf along with other elements confirms the integration of the metal-organic framework onto the magnetic core.

3.2 Catalytic Activity and Optimization

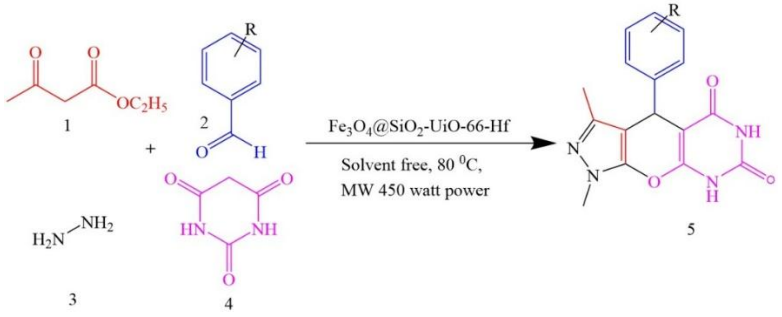

Figure 5 . Synthesis of Dihydropyrazolo[4',3':5,6]pyrano[2,3-d]pyrimidine−5,7− diones Derivatives 5 in the presence of Fe_3O_4@SiO_2-UiO-66-Hf as a catalyst

In our initial study, we describe condensation of ethyl acetoacetate 1, aromatic aldehydes 2, hydrazine hydrate 3, and barbituric acid 4, in the presence of Fe_3O_4@SiO_2-UiO-66-Hf as a heterogeneous catalyst for the synthesis of Dihydropyrazolo[4',3':5,6]pyrano[2,3-d]pyrimidine Derivatives 5 (Fig. 1).

At first, we tested the reaction between ethyl acetoacetate, Benzaldehyde, hydrazine hydrate, and barbituric acid in the presence of of Fe_3O_4@SiO_2-UiO-66-Hf as a catalyst in different amount of catalyst, microwave irradiation power and temperature to optimize the reaction conditions **(Table 1).**

Table 1 The optimization of reaction conditions for the synthesis of 5a.

Entry	Catalyst Amount (g)	Microwave Power (W)	Time (min)	Yield* (%)
1	0.00	300	10	35
2	0.05	300	10	57
3	0.10	300	10	86
4	0.15	300	10	87
5	0.20	300	10	88
6	0.10	150	10	65
7	0.10	450	10	90
8	0.10	600	10	80
9	0.10	450	4	68

10	0.10	450	6	90
11	0.10	450	8	91
* Isolated yield. Reaction conditions ethyl acetoacetate (1 mmol),, aromatic aldehydes (1 mmol), hydrazine hydrate (1 mmol), and barbituric acid (1 mmol) in the presence of Fe_3O_4@SiO_2-UiO-66-Hf				

In the absence of a catalyst, the yield was limited to 35%, underscoring the catalytic function of Hf-MMOF-1. Doubling the catalyst amount from 0.05 g to 0.10 g increased the yield from 57% to 86%. Further increases in catalyst quantity offered negligible advantages, suggesting that 0.10 g is the saturation point. With 0.10 g of catalyst and a reaction time of 10 minutes, a power of 150 W resulted in a 65% yield. The yield reached its maximum at 90% with 450 W, but dropped to 80% at 600 W, likely due to overheating. Under optimal conditions (0.10 g catalyst, 450 W), a 4-minute reaction produced a 68% yield, while extending the time to 6 minutes achieved a 90% yield. Longer reaction times provided little additional benefit, making 6 minutes the ideal duration. As shown in Table 1, the best result was obtained at 0.1 g load of catalyst, at 450 W power of microwave irradiation for 6 min.

After optimizing the reaction conditions, we used several aromatic aldehydes (containing electron rich or electron deficient substituent) for the synthesis of other derivatives in solvent free condition at 80 ^{0}C, 0.1 g load of catalyst, at 450 W power of microwave irradiation for 6 min, as shown results in Table 2. After completion of the reaction which was monitored by TLC, the mixture was dissolved in hot ethanol, the heterogeneous solid catalyst was removed easily by external permanent magnet, and after cooling of the filtrate, the pure crystals of products were obtained as mentioned in Table 2.

Table 2. Substrate scope for the synthesis of Dihydropyrazolo[4',3':5,6]pyrano[2,3-d]pyrimidine−5,7−diones Derivatives using Hf-MMOF catalyst

Entry	Ar	Product	Yield (%)	M.P. ^{0}C (observed)	M.P. ^{0}C (Literature)	References
1	C_6H_5	5a	89.3	214-216	216-218	[22]
2	4-Cl-C_6H_4	5b	91.2	222-224	221-223	[22]
3	4-NO_2-C_6H_4	5c	86.9	222-223	221-223	[23]
4	3-NO_2-C_6H_4	5d	87.7	198-200	197-199	[23]
5	4-OCH_3-C_6H_4	5e	87.7	190	189-190	[22]
6	2-OH-C_6H_4	5f	90.8	212-213	210-213	[22]
7	4-OH-C_6H_4	5g	85.4	256-258	254-256	[23]
8	2-Cl-C_6H_4	5h	86.8	152	151-152	[23]
9	2-CH_3-C_6H_4	5i	93.6	238-240	239-241	[23]
10	4-CH_3--C_6H_4	5j	91.0	228-230	224-227	[22]

The acid catalyst can be reactivated by stirring 24 hrs in diluted H_2SO_4 acid solution, followed by washed with water and acetone, and dry at 150 ^{0}C in hot air oven for 24 hrs. and then reused without noticeable loss of reactivity.

3.3 Catalyst Recyclability

As shown in Table 3, the recovered could be Fe_3O_4@SiO_2-UiO-66-Hf recycled for five times without any significant loss of yields.

Table 3. Synthesis of Dihydropyrazolo[4',3':5,6]pyrano[2,3-d]pyrimidine−5,7− diones 5a with recycled Fe_3O_4@SiO_2-UiO-66-Hf as a catalyst

	1st run	2nd run	3rd run	4th run	5th run
Yield (%)	89	88	85	82	80

Recycle experiments were carried out at 1 mmole of on ethyl acetoacetate, banzaldehyde, hydrazine hydrate and barbituric acid in the presence of Fe_3O_4@SiO_2-UiO-66-Hf at 6 min irradiation duration.

Fe_3O_4@SiO_2@UiO-66(Hf) was reused for five cycles with only a marginal decrease in yield (from 89% to 80%), indicating robust stability and reusability.

3.4 Comparative Performance

Synthesis of Dihydropyrazolo[4',3':5,6]pyrano[2,3-d]pyrimidine−5,7− diones has been reported under different conditions in the literature, as shown in Table 4. In contrast with other existing methods, the MMOF catalyst under microwave irradiation showed superior reaction rates, higher yields, and easier recovery, easy work-up, and green condition are the advantages of current methodology, highlighting its practical advantages.

Table 4. Comparison of Synthesis of Dihydropyrazolo[4',3':5,6]pyrano[2,3-d]pyrimidine−5,7− diones

Entry	Catalyst	Reaction Time	Catalyst Amount	Yield (%)	Reaction Conditions	Reference
1	DABCO	20 min	20 mol%	95	H_2O, Reflux	[24]
2	Co-MOF@Ag_2O nanocomposite	10 min	20 mol%	92	H_2O, 50°C	[25]
3	Fe_3O_4/Zn-MOF magnetic	20 min	0.1 g	>85	Microwave-assisted, EtOH	[26]
4	BNPs-Caff]HSO_4	40 min	0.1 g	95	H_2O, 50°C	[27]
5	TiO_2 nanowires	60 min	10 mol%	95	H_2O, Reflux	[28]

Anusandhanvallari
Vol 2024, No.1
August 2024
ISSN 2229-3388

4. Discussion

4.1 Proposed Mechanism

A proposed mechanism for the synthesis of Dihydropyrazolo[4',3':5,6]pyrano[2,3-d]pyrimidine−5,7− diones derivatives 5 is shown in Fig. 2. Initially the Knoevenagel condensation of aldehyde 1 and barbituric acid 2 produces intermedidate 3. Hydrazine hydrate 4 initially reacts with ethyl acetoacetate 5 through nucleophilic acyl substitution, followed by cyclization to generate the pyrazolone intermediate 6. Michael addition intermediate 3 to product 6 gives the intermediate 7. The resulting adduct undergoes intramolecular cyclization and subsequent tautomerization, yielding the final product 8 tricyclic fused system. The catalytic cycle likely initiates with Lewis acid activation of the carbonyl groups by Hf centers in the MOF, facilitating reaction proceed.

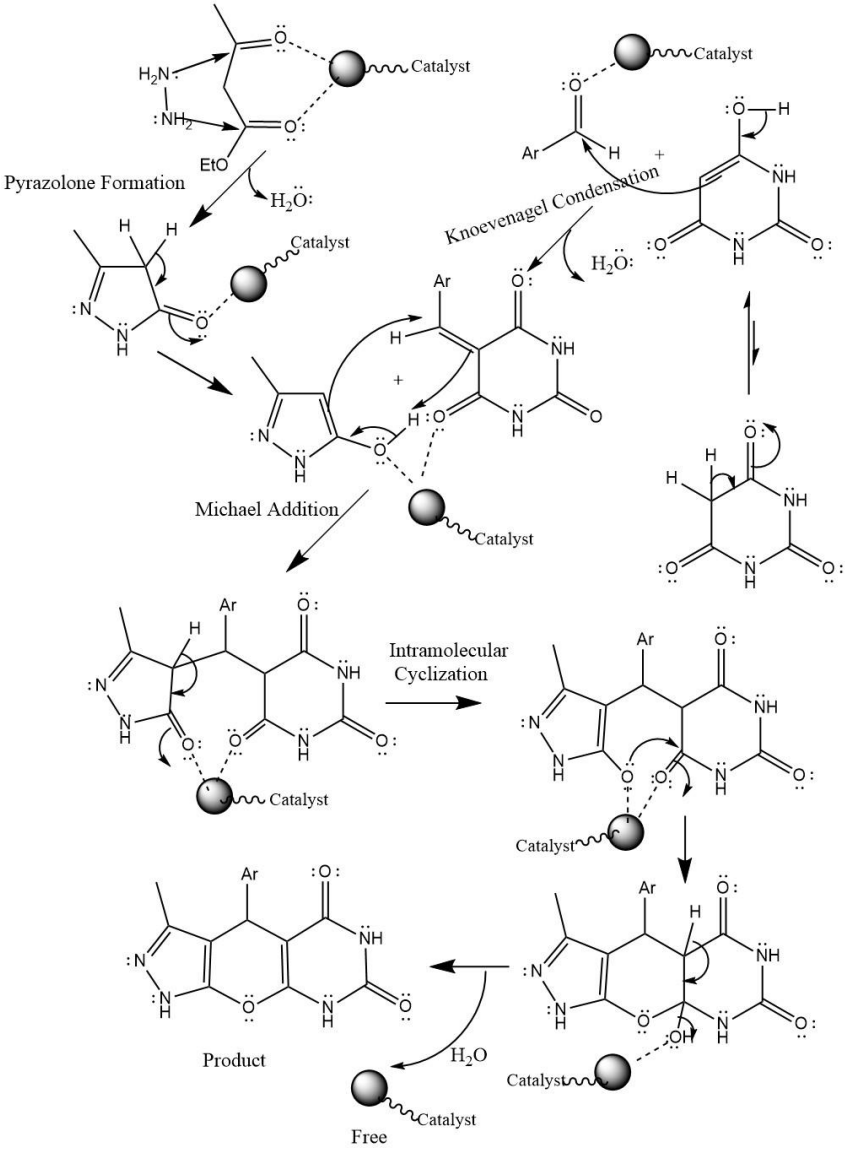

Figure 5 . A proposed mechanism for the synthesis of Dihydropyrazolo[4',3':5,6]pyrano[2,3-d]pyrimidine−5,7− diones derivatives 5.

4.2 Structure–Activity Relationships

The combination of magnetic Fe3O4 and UiO-66(Hf) provides synergistic effects: magnetic separation efficiency coupled with high surface area and Lewis acidity. The silica shell stabilizes the magnetic core and promotes MOF growth, enhancing catalyst durability. Porosity ensures substrate accessibility, critical for high catalytic turnover.

4.3 Green Chemistry Considerations

The solvent-free microwave-assisted protocol minimizes waste and energy consumption. Catalyst recyclability reduces material usage. The heterogeneous system avoids corrosive homogeneous acids, aligning with sustainable synthesis principles.

4.4 Comparison with Literature

This method outperforms many reported approaches in terms of reaction time, yield, and catalyst recovery. The use of a Hf-based MMOF catalyst is novel in this context, providing a robust platform for other heterocyclic syntheses.

5. Analytical data of some selected compounds

5.1 Compound 5a :3-Methyl-4-phenyl-4,8-dihydropyrazolo[4',3':5,6]pyrano[2,3-d]pyrimidine-5,7(1H,6H)-dione

Physical State : White solid

Yield: 89-95%

M.P.: 238-240 ^{0}C

^{1}H NMR (400 MHz, DMSO-d_6): δ 2.13 (s, 3H, CH_3), 5.53 (s, 1H, CH), 7.09 (d, 2H, Ar), 7.22 (d, 2H, Ar), 7.25 (t, 1H, Ar), 10.220 (br s, 2H, NH), 13.25 (br s, 1H, NH) ppm

^{13}C NMR (500 MHz, DMSO-d_6): δ 165.8, 164.8, 160, 150.3, 142.0, 143.6, 127.8, 126.5, 125.4, 105.5, 91.9, 30.48, 10.12 ppm

FT-IR (KBr): 3317, 3122, 3017, 1697, 1594, 1348, 1296, 970, 773 cm^{-1}

Mass (ESI-MS): 310.313 (100%)

5.2 Compound 5b: 4-(4-Chlorophenyl)-3-methyl-4,8-dihydropyrazolo[4',3':5,6]pyrano[2,3-d]pyrimidine-5,7(1H,6H)-dione

Physical State: White solid

Yield: 91-95 %

M.P.: 222-224 ^{0}C

^{1}H NMR (400 MHz, DMSO-d_6): δ 2.32 (s, 3H, CH_3), 5.60 (s, 1H, CH), 7.78 (d, 2H, Ar), 7.92 (d, 2H, Ar), 10.2 (br s, 2H, NH) ppm

^{13}C NMR (500 MHz, DMSO-d_6): δ 163.1, 160.5, 160.33, 150.52, 142.9, 141.45, 130.01, 128.6, 127.6, 109.0, 91.4, 56.0, 9.9 ppm

FT-IR (KBr): 3312, 3120, 1705, 1582, 1299, 1042, 810, 732 cm^{-1}

Mass (ESI-MS): 330.1005 (100%)

6. Conclusion

A microwave-facilitated, heterogeneous catalytic protocol utilizing Fe3O4@SiO2@UiO-66(Hf) MMOFs was successfully developed for the synthesis of dihydropyrazolo[4',3':5,6]pyrano[2,3-d]pyrimidine derivatives. The catalyst demonstrated high activity, selectivity, and recyclability under green, solvent-free conditions. This study contributes a sustainable and efficient methodology for constructing complex heterocycles with potential pharmaceutical relevance. Future work will explore catalyst modification to expand substrate scope and mechanistic elucidation via spectroscopic techniques.

7. Acknowledgments

We gratefully acknowledge the support from the School of science, YCMOU University, Nashik Maharashtra from India.

8. References

1. Tran, T. N., & Henary, M. (2022). Synthesis and Applications of Nitrogen-Containing Heterocycles as Antiviral Agents. Molecules, 27(9), 2700. https://doi.org/10.3390/molecules27092700
2. Sachdeva, H., Khatik, N., Sharma, K., Khandelwal, A. R., Saquib, M., Meena, R., & Khaturia, S. (2022). Oxygen- and Sulphur-Containing Heterocyclic Compounds as Potential Anticancer Agents. Applied Biochemistry and Biotechnology, 194(12), 6438–6467. https://doi.org/10.1007/s12010-022-04099-w
3. Dinodia, M. (2023). N-heterocycles: Recent Advances in Biological Applications. Mini-Reviews in Organic Chemistry, 20(7), 735–747. https://doi.org/10.2174/1570193x19666211231101747
4. Ali, T. E., Bakhotmah, D. A., & Assiri, M. A. (2020). Synthesis of some new functionalized pyrano[2,3-c]pyrazoles and pyrazolo[4′,3′:5,6] pyrano[2,3-d]pyrimidines bearing a chromone ring as antioxidant agents. Synthetic Communications, 50(21), 3314–3325. https://doi.org/10.1080/00397911.2020.1800744
5. Zhang, J., Song, H., Cui, R., Deng, C., & Yousif, Q. A. (2020). SCMNPs@Urea/Py-CuCl2: a recyclable catalyst for the synthesis of pyrano[2,3-d]pyrimidinone and pyrano[2,3-d] pyrimidine-2,4,7-trione derivatives. Journal of Coordination Chemistry, 73(4), 558–578. https://doi.org/10.1080/00958972.2020.1737681
6. Ostadzadeh, H., & Kiyani, H. (2022). Multicomponent Synthesis of Tetrahydrobenzo[b]Pyrans, Pyrano[2,3-d]Pyrimidines, and Dihydropyrano[3,2-c]Chromenes Catalyzed by Sodium Benzoate. Polycyclic Aromatic Compounds, 43(10), 9318–9337. https://doi.org/10.1080/10406638.2022.2162091
7. Kohli, S., Rawat, M., Rawat, S., Saraswat, V., Rathee, G., & Nagar, S. (2024). Advancement in Heterogeneous Catalysts for the Synthesis of Benzothiazole Derivatives. ChemistrySelect, 9(42). https://doi.org/10.1002/slct.202402856
8. Chen, X., Cui, Y., Liu, Y., Gong, W., Jiang, H., & Hou, B. (2017). Boosting Chemical Stability, Catalytic Activity, and Enantioselectivity of Metal-Organic Frameworks for Batch and Flow Reactions. Journal of the American Chemical Society, 139(38), 13476–13482. https://doi.org/10.1021/jacs.7b06459
9. Wang, L., Liu, H., Li, S., Hou, H., Qiao, W., & Wu, J. (2023). Synergistic Effects of Lewis Acid-Base Pair Sites─Hf-MOFs with Functional Groups as Distinguished Catalysts for the Cycloaddition of Epoxides with CO2. Inorganic Chemistry, 62(9), 3817–3826. https://doi.org/10.1021/acs.inorgchem.2c04078

10. Cui, H., Fu, M., Yuan, B., & Huo, J. (2017). The fabrication of magnetic metal-organic frameworks composites and their application in environment. SCIENTIA SINICA Chimica, 47(7), 830–843. https://doi.org/10.1360/n032016-00199
11. Kandelous, Y. M., Nikpassand, M., & Fekri, L. Z. (2024). Recent Focuses in the Syntheses and Applications of Magnetic Metal-Organic Frameworks. Topics in Current Chemistry (Cham), 382(4). https://doi.org/10.1007/s41061-024-00475-8
12. Kumar, S., Kumar, M., & Singh, A. (2021). Synthesis and characterization of iron oxide nanoparticles (Fe2O3, Fe3O4): a brief review. Contemporary Physics, 62(3), 144–164. https://doi.org/10.1080/00107514.2022.2080910
13. Camacho-Fernández, J. C., González-Quijano, G. K., Séverac, C., Dague, E., Gigoux, V., Santoyo-Salazar, J., & Martinez-Rivas, A. (2021). Nanobiomechanical behavior of Fe3O4@SiO2 and Fe3O4@SiO2–NH2 nanoparticles over HeLa cells interfaces. Nanotechnology, 32(38), 385702. https://doi.org/10.1088/1361-6528/ac0a13
14. Sembiring, T., Kurniawan, B., Nurbillah, A., Lubis, H., Lubis, R. Y., Sitinjak, N. R. L., & Noer, Z. (2024). Synthesis and characterization of Magnetic Fe3O4/SiO2 composite for Environmental Sanitation. Journal of Physics: Conference Series, 2733(1), 012027. https://doi.org/10.1088/1742-6596/2733/1/012027
15. Ediati, R., Mukminin, A., Nugroho, K. A., Zulfa, L. L., Kusumawati, Y., Nadjib, M., & Sulistiono, D. O. (2019). One-pot solvothermal synthesis and characterization of UiO-66/HKUST-1 composites. IOP Conference Series: Materials Science and Engineering, 578(1), 012072. https://doi.org/10.1088/1757-899x/578/1/012072
16. Petreanu, I., Niculescu, V.-C., Enache, S., Iacob, C., & Teodorescu, M. (2022). Structural Characterization of Silica and Amino-Silica Nanoparticles by Fourier Transform Infrared (FTIR) and Raman Spectroscopy. Analytical Letters, ahead-of-print(ahead-of-print), 390–403. https://doi.org/10.1080/00032719.2022.2083144
17. Dawn, R., Zzaman, M., Faizal, F., Kiran, C., Kumari, A., Shahid, R., Panatarani, C., Joni, I. M., Verma, V. K., Sahoo, S. K., Amemiya, K., & Singh, V. R. (2022). Origin of Magnetization in Silica-coated Fe3O4 Nanoparticles Revealed by Soft X-ray Magnetic Circular Dichroism. Brazilian Journal of Physics, 52(3). https://doi.org/10.1007/s13538-022-01102-x
18. Lyu, J., Bai, P., Xiao, Z., Liu, H., Guo, X., Zhang, J., & Zeng, Z. (2017). Metal–Organic Framework UiO-66 as an Efficient Adsorbent for Boron Removal from Aqueous Solution. Industrial & Engineering Chemistry Research, 56(9), 2565–2572. https://doi.org/10.1021/acs.iecr.6b04066
19. Chen, R., Liu, Z., Wang, J., Tao, C.-A., Zhang, Z., & Chen, X. (2019). Layer-by-Layer Fabrication of Core-Shell Fe3O4@UiO-66-NH2 with High Catalytic Reactivity toward the Hydrolysis of Chemical Warfare Agent Simulants. ACS Applied Materials & Interfaces, 11(46), 43156–43165. https://doi.org/10.1021/acsami.9b14099
20. Semivrazhskaya, O. O., Ranocchiari, M., Sushkevich, V. L., Van Bokhoven, J. A., Salionov, D., Bjelić, S., Nachtegaal, M., Verel, R., Clark, A. H., & Casati, N. P. M. (2023). Deciphering the Mechanism of Crystallization of UiO-66 Metal-Organic Framework. Small, 19(52). https://doi.org/10.1002/smll.202305771
21. Asab, G., Zereffa, E. A., & Abdo Seghne, T. (2020). Synthesis of Silica-Coated Fe3O4 Nanoparticles by Microemulsion Method: Characterization and Evaluation of Antimicrobial Activity. International Journal of Biomaterials, 2020(3–4), 1–11. https://doi.org/10.1155/2020/4783612
22. Bakherad, M., Gholizadeh, M., Keivanloo, A., Javanmardi, M., & Doosti, R. (2016). Using magnetized water as a solvent for a green, catalyst-free, and efficient protocol for the synthesis of pyrano[2,3-c]pyrazoles and pyrano[4′,3′:5,6]pyrazolo [2,3-d]pyrimidines. Research on Chemical Intermediates, 43(2), 1013–1029. https://doi.org/10.1007/s11164-016-2680-y

23. Momeni, S., & Ghorbani-Vaghei, R. (2024). Copper Immobilized on Modified LDHs as a Novel Efficient Catalytic System for Three-Component Synthesis of Pyrano[2,3-d]pyrimidine and pyrazolo[4',3':5,6]pyrano[2,3-d]pyrimidine Derivatives. ACS Omega, 9(9), 10332–10342. https://doi.org/10.1021/acsomega.3c07913
24. Heravi, M. M., Mousavizadeh, F., Tajbakhsh, M., & Ghobadi, N. (2014). ChemInform Abstract: A Green and Convenient Protocol for the Synthesis of Novel Pyrazolopyranopyrimidines via a One-Pot, Four-Component Reaction in Water. ChemInform, 45(28), no. https://doi.org/10.1002/chin.201428171
25. Hootifard, G., Sheikhhosseini, E., Ahmadi, S. A., & Yahyazadehfar, M. (2023). Synthesis and characterization of Co-MOF@Ag2O nanocomposite and its application as a nano-organic catalyst for one-pot synthesis of pyrazolopyranopyrimidines. Scientific Reports, 13(1). https://doi.org/10.1038/s41598-023-44667-6
26. Bashar, B. S., Kareem, H. A., Hasan, Y. M., Ahmad, N., Alshehri, A. M., Al-Majdi, K., Hadrawi, S. K., Al Kubaisy, M. M. R., & Qasim, M. T. (2022). Application of novel Fe3O4/Zn-metal organic framework magnetic nanostructures as an antimicrobial agent and magnetic nanocatalyst in the synthesis of heterocyclic compounds. Frontiers in Chemistry, 10. https://doi.org/10.3389/fchem.2022.1014731
27. Rostami, A., Darvishi, N., Navasi, Y., Pourshiani, O., & Saadati, S. (2017). Magnetic nanoparticle-supported DABCO tribromide: a versatile nanocatalyst for the synthesis of quinazolinones and benzimidazoles and protection/deprotection of hydroxyl groups. New Journal of Chemistry, 41(17), 9033–9040. https://doi.org/10.1039/c7nj00479f
28. Farooq, S., & Ngaini, Z. (2020). Chalcone Derived Pyrazole Synthesis via One-pot and Two-pot Strategies. Current Organic Chemistry, 24(13), 1491–1506. https://doi.org/10.2174/1385272824999200714101420